Pergamon

Int. J. Solids Structures Vol. 31, No. 9, pp. 1279–1290, 1994

0020–7683/94 $6.00 + .00

0020–7683(93)E0034–F

ON THE PROBLEM OF A DETACHED ANCHOR PLATE EMBEDDED IN A CRACK

A. P. S. SELVADURAI
Department of Civil Engineering and Applied Mechanics, McGill University, Montreal, Québec H3A 2K6, Canada

(*Received* 8 *July* 1993; *in revised form* 3 *November* 1993)

Abstract—The present paper examines the elastostatic problem related to the axisymmetric indentation of the single surface of a penny-shaped crack by a rigid disc anchor. The governing integral equation is solved in a numerical fashion to evaluate the axial stiffness characteristics of the indenting disc anchor and the stress intensity factors at the tip of the penny-shaped crack.

INTRODUCTION

The theory of a disc-shaped anchoring element or foundation has been studied quite extensively in the context of the modelling of anchoring devices, *in situ* plate load tests and deep foundations embedded in geological media [see, for example, Selvadurai (1976), (1979), (1980), (1984), (1993); Rowe and Booker (1979); Selvadurai and Nicholas (1979); Selvadurai and Au (1986); Rowe and Davis (1982); Selvadurai *et al.* (1990)]. In particular, the class of solutions based on the classical theory of elasticity have found extensive applications in the modelling of anchor behaviour related to geomaterials such as soft rocks, overconsolidated clays, etc. While the conventional elastostatic studies in this area have focused on isolated disc anchors with perfect interface bonding, the subject matter has been extended to include the influence of debonding (Hunter and Gamblen, 1974; Keer, 1975) and crack development (Selvadurai, 1989) at the boundaries of the circular anchor. The paper by Selvadurai (1989) considered the problem of the axial loading behaviour of a rigid circular anchor plate which was embedded in bonded contact with the surfaces of a penny-shaped crack. The development of such cracks was attributed to the use of expansive cementaceous grout material which are used to create the injection anchor regions in soft rock masses. Similar crack development is feasible either during the penetration of single helix ground anchors or during a plate loading test conducted at the base of a borehole. The modelling of the boundary fracture problem examined by Selvadurai (1989) focused on the idealized problem where, although boundary fracture was initiated at the perimeter of the circular anchor, the plane faces of the anchor remained *bonded* to the geological medium. This elastostatic model was intended to serve as a suitable approximation for either deeply embedded anchors with open boundary cracks where influence of self-weight of the geological medium would ensure bonded contact at both interfaces even during application of the anchor loads or for situations where high interface strength would ensure bonding at both plane faces of the anchor. In this study the more realistic situation is examined where the anchor plate experiences debonding at one of the plane faces, due to the application of the axial anchor load P (Fig. 1). Attention is therefore focused on the axisymmetric smooth indentation of the single surface of a penny-shaped crack by a rigid circular anchor plate. The assumption of smooth contact at the anchor plate–elastic medium interface is an idealization since in practice, such interfaces could exhibit a variety of contact conditions ranging from complete bonding to smooth contact with Coulomb friction or finite friction occupying an intermediate position. For the purposes of this paper a smooth contact is assumed with the understanding that the compliance of the anchor plate is at its greatest when the interface bonding condition is relaxed. The mathematical analysis of the elastostatic anchor problem utilizes a Hankel transform approach which yields a system of three coupled integral equations. These in turn are

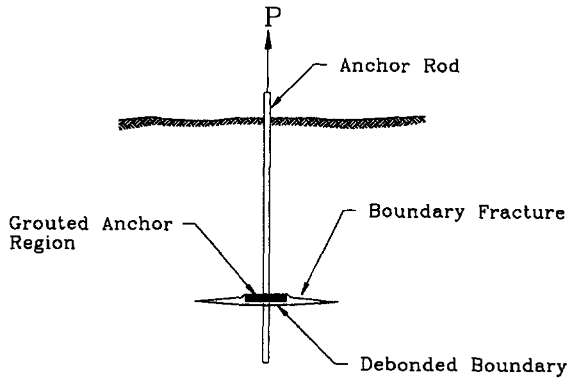

Fig. 1. Partially bonded plate anchor embedded in a penny-shaped crack.

reduced to a single Fredholm integral equation of the second kind which is solved in a numerical fashion to generate results of engineering interest. These include the axial stiffness of the anchor plate and stress intensity factors at the boundary of the circular crack.

FUNDAMENTAL EQUATIONS

The problem examined is shown in Fig. 2. A rigid circular plate anchor of radius a is axisymmetrically located in a penny-shaped crack of radius b. The application of an axisymmetric load P induces a rigid displacement Δ within the smooth indentation region. Since the anchor problem exhibits a state of axial symmetry, it is convenient to employ the strain potential solution representation for elastostatic problems given by Love (1927). It can be shown that the solution to the displacement equations of equilibrium can be expressed in terms of a single function $\varphi(r, z)$ which satisfies the equation

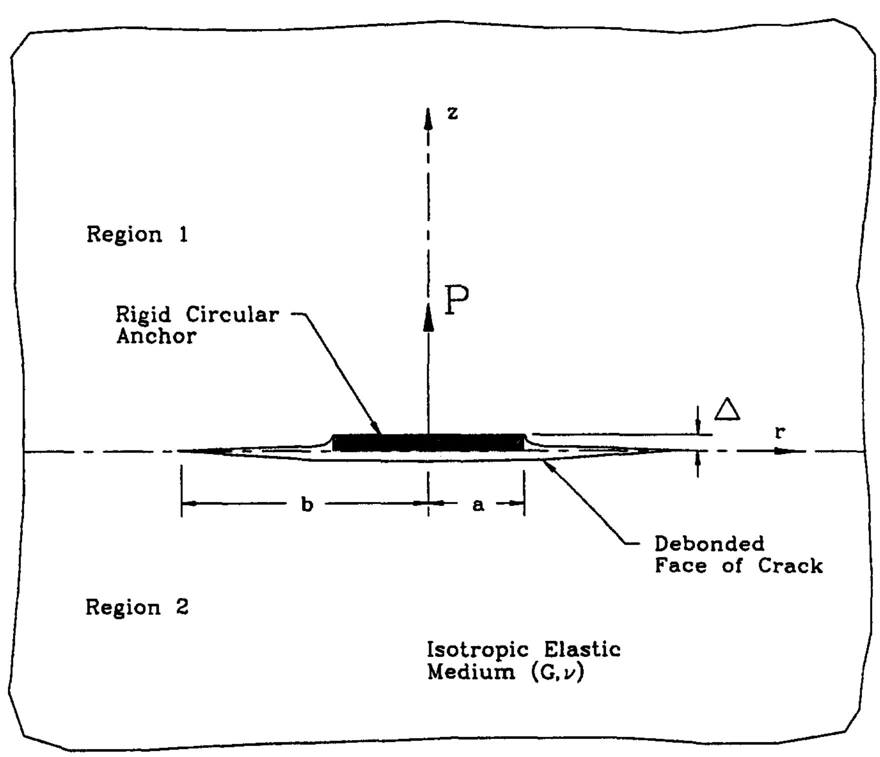

Fig. 2. The detached plate anchor problem.

$$\nabla^2\nabla^2\varphi(r,z) = 0, \tag{1}$$

where

$$\nabla^2 = \frac{\partial^2}{\partial r^2} + \frac{1}{r}\frac{\partial}{\partial r} + \frac{\partial^2}{\partial z^2} \tag{2}$$

is the axisymmetric form of Laplace's operator in cylindrical polar coordinates. In order to derive the integral equations governing the disc anchor problem we seek solutions of eqn (1) which are based on Hankel transform developments of the governing equation (Sneddon, 1977) and applicable to the regions 1 ($0 \leqslant z < \infty$) and 2 ($-\infty < z \leqslant 0$) which are defined in Fig. 2, i.e.

$$\varphi^{(1)}(r,z) = \int_0^\infty [A(\zeta)+B(\zeta)z]\,\mathrm{e}^{-\zeta z}J_0(\zeta r)\,\mathrm{d}\zeta \tag{3}$$

$$\varphi^{(2)}(r,z) = \int_0^\infty [C(\zeta)+D(\zeta)z]\,\mathrm{e}^{\zeta z}J_0(\zeta r)\,\mathrm{d}\zeta, \tag{4}$$

where $A(\zeta)\ldots D(\zeta)$ are arbitrary functions which should be determined by satisfying the mixed boundary conditions at the faces of the cracked region and continuity conditions at the intact region exterior to the crack occupying the plane $z = 0$. The superscripts (1) and (2) refer to halfspace regions 1 and 2, respectively. The relevant displacement and stress components applicable to the regions 1 and 2 can be obtained from the expressions

$$2G_\alpha u_r^{(\alpha)} = -\frac{\partial^2\varphi^{(\alpha)}}{\partial r\,\partial z} \tag{5}$$

$$2G_\alpha u_z^{(\alpha)} = 2(1-\nu_\alpha)\nabla^2\varphi^{(\alpha)} - \frac{\partial^2\varphi^{(\alpha)}}{\partial z^2} \tag{6}$$

$$\sigma_{zz}^{(\alpha)} = \frac{\partial}{\partial z}\left\{(2-\nu_\alpha)\nabla^2\varphi^{(\alpha)} - \frac{\partial^2\varphi^{(\alpha)}}{\partial z^2}\right\} \tag{7}$$

$$\sigma_{rz}^{(\alpha)} = \frac{\partial}{\partial r}\left\{(1-\nu_\alpha)\nabla^2\varphi^{(\alpha)} - \frac{\partial^2\varphi^{(\alpha)}}{\partial z^2}\right\}, \tag{8}$$

where $\alpha = 1, 2$.

THE DETACHED ANCHOR PLATE PROBLEM

We consider the detached anchor plate problem where a rigid circular anchor plate indents a single surface of a penny-shaped crack. The interface between the anchor plate and the surface of the crack is assumed to be smooth. The detached surface of the crack is assumed to be traction free. The problem is considered to be axisymmetric where an axial load P acting on the anchor plate induces a rigid displacement Δ. The mixed boundary conditions applicable to both surfaces of the crack are as follows:

$$u_z^{(1)}(r,0) = \Delta, \quad 0 \leqslant r \leqslant a \tag{9}$$

$$\sigma_{zz}^{(1)}(r,0) = 0, \quad a < r < b \tag{10}$$

$$\sigma_{rz}^{(1)}(r,0) = 0, \quad 0 < r < b \tag{11}$$

$$\sigma_{zz}^{(2)}(r,0) = 0, \quad 0 < r < b \tag{12}$$

$$\sigma_{rz}^{(2)}(r,0) = 0, \quad 0 < r < b. \tag{13}$$

The continuity conditions applicable to the exterior region containing the penny-shaped crack are given by

$$u_z^{(1)}(r,0) = u_z^{(2)}(r,0), \quad b \leqslant r < \infty \tag{14}$$

$$u_r^{(1)}(r,0) = u_r^{(2)}(r,0), \quad b \leqslant r < \infty \tag{15}$$

$$\sigma_{zz}^{(1)}(r,0) = \sigma_{zz}^{(2)}(r,0), \quad b < r < \infty \tag{16}$$

$$\sigma_{rz}^{(1)}(r,0) = \sigma_{rz}^{(2)}(r,0), \quad b < r < \infty. \tag{17}$$

Considering the boundary conditions and continuity conditions (9)–(17) it can be shown that

$$H_0[\zeta^{-1}\{N(\zeta)+\zeta(1-2\nu)B(\zeta)\};r] = -2G\Delta; \quad 0 \leqslant r \leqslant a \tag{18}$$

$$H_0[N(\zeta);r] = 0, \quad a < r < b \tag{19}$$

$$H_1[\{N(\zeta)-\zeta B(\zeta)\};r] = 0, \quad 0 < r < b \tag{20}$$

$$H_0[P(\zeta);r] = 0, \quad 0 < r < b \tag{21}$$

$$H_1[Q(\zeta);r] = 0, \quad 0 < r < b \tag{22}$$

$$H_0[\zeta^{-1}\{N(\zeta)+\zeta(1-2\nu)B(\zeta)+2(1-\nu)P(\zeta)+(1-2\nu)Q(\zeta)\};r] = 0, \quad b \leqslant r < \infty \tag{23}$$

$$H_1[\zeta^{-1}\{(1-2\nu)P(\zeta)+2(1-\nu)Q(\zeta)+N(\zeta)-2(1-\nu)\zeta B(\zeta)\};r] = 0, \quad b < r < \infty \tag{24}$$

$$H_0[\{P(\zeta)-N(\zeta)\};r] = 0, \quad b < r < \infty \tag{25}$$

$$H_1[\{Q(\zeta)-N(\zeta)+\zeta B(\zeta)\};r] = 0, \quad b < r < \infty, \tag{26}$$

where

$$\zeta[\zeta A(\zeta)+(1-2\nu)B(\zeta)] = N(\zeta) \tag{27}$$

$$\zeta[(1-2\nu)D(\zeta)-\zeta C(\zeta)] = P(\zeta) \tag{28}$$

$$\zeta[\zeta C(\zeta)+2\nu D(\zeta)] = Q(\zeta) \tag{29}$$

and $H_n[\Omega(\zeta);r]$ is the Hankel transform of order n defined by

$$H_n[\Omega(\zeta);r] = \int_0^\infty \zeta\Omega(\zeta)J_n(\zeta r)\,\mathrm{d}\zeta. \tag{30}$$

Considering (20) we can show that

$$N(\zeta)-\zeta B(\zeta) = \int_b^\infty rg(r)J_1(\zeta r)\,\mathrm{d}r, \tag{31}$$

where $g(r)$ is an unknown function defined in $r \in (b, \infty)$. Also from (26) we have

$$H_1[Q(\zeta);r] = g(r), \quad b < r < \infty. \tag{32}$$

Considering (22) and (32) we have

$$Q(\zeta) = \int_b^\infty rg(r)J_1(\zeta r)\,\mathrm{d}r = N(\zeta)-\zeta B(\zeta). \tag{33}$$

The eqns (18), (23) and (24) can be written as

$$H_0[\zeta^{-1}N(\zeta);r] = -\frac{\Delta G}{(1-\nu)} + \frac{(1-2\nu)}{(2-2\nu)} H_0[\zeta^{-1}Q(\zeta);r] = G_1(r), \quad 0 < r < a \tag{34}$$

$$H_0[\zeta^{-1}N(\zeta);r] = -H_0[\zeta^{-1}P(\zeta);r] = G_2(r), \quad b < r < \infty \tag{35}$$

$$H_1[\zeta^{-1}N(\zeta);r] = \frac{4(1-\nu)}{(1-2\nu)} H_1[\zeta^{-1}Q(\zeta);r] + H_1[\zeta^{-1}P(\zeta);r], \quad b < r < \infty. \tag{36}$$

We now assume that $N(\zeta)$ admits a representation

$$H_0[N(\zeta);r] = \begin{cases} f_1(r), & 0 < r < a \\ f_2(r), & b < r < \infty. \end{cases} \tag{37}$$

Alternatively from the Hankel inversion theorem we have

$$N(\zeta) = \int_0^a r f_1(r) J_0(\zeta r) + \int_b^\infty r f_2(r) J_0(\zeta r)\, \mathrm{d}r. \tag{38}$$

Following Selvadurai and Singh (1985), the solution of the system of triple integral equations (19), (34) and (35) can be written as

$$F_1(r) + \frac{2}{\pi}\int_b^\infty \frac{sF_2(s)\,\mathrm{d}s}{(s^2-r^2)} = g_1(r), \quad 0 < r < a \tag{39}$$

$$F_2(r) + \frac{2r}{\pi}\int_0^a \frac{F_1(s)\,\mathrm{d}s}{(r^2-s^2)} = g_2(r), \quad b < r < \infty, \tag{40}$$

where

$$g_1(r) = \frac{\mathrm{d}}{\mathrm{d}r}\int_0^r \frac{tG_1(t)\,\mathrm{d}t}{(r^2-t^2)^{1/2}} \tag{41}$$

$$g_2(r) = -\frac{\mathrm{d}}{\mathrm{d}r}\int_r^\infty \frac{tG_2(t)\,\mathrm{d}t}{(t^2-r^2)^{1/2}} \tag{42}$$

$$F_1(s) = \int_s^a \frac{rf_1(r)\,\mathrm{d}r}{(r^2-s^2)^{1/2}}, \quad 0 < s < a \tag{43}$$

$$F_2(s) = \int_b^s \frac{rf_2(r)\,\mathrm{d}r}{(s^2-r^2)^{1/2}}, \quad b < s < \infty. \tag{44}$$

Using the results

$$\int_0^r \frac{tJ_0(\zeta t)}{(r^2-t^2)^{1/2}} = \frac{\sin(\zeta r)}{\zeta}, \qquad \int_r^\infty \frac{tJ_0(\zeta t)\,\mathrm{d}t}{(t^2-r^2)^{1/2}} = \frac{\cos(\zeta r)}{\zeta}, \tag{45}$$

the results (41) and (42) can be written as

$$g_1(r) = -\frac{\Delta G}{(1-\nu)} + \frac{(1-2\nu)}{(2-\nu)}\int_0^\infty Q(\zeta)\cos(\zeta r)\,\mathrm{d}\zeta, \quad 0 < r < a \tag{46}$$

$$g_2(r) = -\int_0^\infty P(\zeta)\sin(\zeta r)\,d\zeta, \quad b < r < \infty. \tag{47}$$

Also, from (31) we have

$$N(\zeta) = \zeta B(\zeta) + \int_b^\infty u g(u) J_1(\zeta u)\,du. \tag{48}$$

From (36) and (48) and the condition

$$\int_0^\infty J_1(\zeta r)J_1(\zeta u)\,d\zeta = \frac{2ru}{\pi}\int_{\max(r,u)}^\infty \frac{d\omega}{\omega^2[(\omega^2-r^2)(\omega^2-u^2)]^{1/2}} \tag{49}$$

it can be shown that

$$\int_r^\infty \frac{S(\omega)\,d\omega}{\omega^2[\omega^2-r^2]^{1/2}} = \frac{\pi}{2r}\int_0^\infty [P(\zeta)-B(\zeta)]J_1(\zeta r)\,d\zeta + \frac{2\pi(1-\nu)}{r(1-2\nu)}\int_0^\infty Q(\zeta)J_1(\zeta r)\,d\zeta, \quad b < r < \infty, \tag{50}$$

where

$$S(\omega) = \int_b^\omega \frac{u^2 g(u)\,du}{(\omega^2-u^2)^{1/2}}, \quad b < \omega < \infty. \tag{51}$$

The eqns (43), (44) and (51) are of the Abel-type; consequently we have

$$f_1(r) = \frac{-2}{\pi r}\frac{d}{dr}\int_r^a \frac{sF_1(s)\,ds}{(s^2-r^2)^{1/2}}, \quad 0 < r < a \tag{52}$$

$$f_2(r) = \frac{2}{\pi r}\frac{d}{dr}\int_b^r \frac{sF_2(s)\,ds}{(r^2-s^2)^{1/2}}, \quad b < r < \infty \tag{53}$$

$$g(u) = \frac{2}{\pi u^2}\frac{d}{du}\int_b^u \frac{\omega S(\omega)\,d\omega}{(u^2-\omega^2)^{1/2}}, \quad b < u < \infty. \tag{54}$$

Substituting the value of $f_1(r)$ and $f_2(r)$ given by (52) and (53) in (38) we have

$$N(\zeta) = \frac{2}{\pi}\left[\int_0^a F_1(s)\cos(s\zeta)\,ds + \int_b^\infty F_2(s)\sin(\zeta s)\,ds\right]. \tag{55}$$

Making use of the inversion theorem we obtain from (21), (25) and (55) an integral expression for $P(\zeta)$ in terms of $F_2(s)$, i.e.

$$P(\zeta) = \frac{2}{\pi}\int_b^\infty F_2(s)\sin(\zeta s)\,ds. \tag{56}$$

Substituting the value of $Q(\zeta)$ defined by (33) and the above value of $P(\zeta)$ in eqns (46) and (47) we have

$$g_1(r) = \frac{-\Delta G}{(1-\nu)} + \frac{(1-2\nu)}{(2-2\nu)} \int_b^\infty g(u)\,\mathrm{d}u, \quad 0 < r < a \tag{57}$$

$$g_2(r) = -F_2(r), \quad b < r < \infty. \tag{58}$$

Hence, from (39) and (40) we obtain a set of triple integral equations of the form

$$T_1(r) + \frac{2}{\pi} \int_b^\infty \frac{u T_2(u)\,\mathrm{d}u}{(u^2 - r^2)} = \frac{-1}{2(1-\nu^2)} + \frac{(1-2\nu)}{(2-2\nu)} \int_b^\infty \frac{S(\omega)\,\mathrm{d}\omega}{\omega^2}, \quad 0 < r < a \tag{59}$$

$$T_2(r) = \frac{-r}{\pi} \int_0^a \frac{T_1(s)}{(r^2 - s^2)}\,\mathrm{d}s, \quad b < r < \infty \tag{60}$$

$$T_3(r) = \frac{(1-2\nu)}{4(1-\nu)} \int_0^a T_1(s)\,\mathrm{d}s, \quad b < r < \infty, \tag{61}$$

where

$$T_1(r) = \frac{F_1(r)}{E\Delta}, \quad T_2(r) = \frac{F_2(r)}{E\Delta}, \quad T_3(r) = \frac{S(r)}{E\Delta} \tag{62}$$

and E is Young's modulus of the medium. The system of triple integral eqns (59)–(61) is equivalent to a single integral equation of the form

$$T_1(r) + \frac{1}{\pi^2} \int_0^a \frac{T_1(s) K_1(r,s)\,\mathrm{d}s}{(r^2 - s^2)} - \frac{(1-2\nu)^2}{8b(1-\nu)^2} \int_0^a T_1(s)\,\mathrm{d}s = -\frac{1}{2(1-\nu^2)}, \quad 0 < r < a, \tag{63}$$

where

$$K_1(r,s) = r \ln\left|\frac{b-r}{b+r}\right| - s \ln\left|\frac{b-s}{b+s}\right|. \tag{64}$$

The problem of the axisymmetric loading of a detached anchor plate embedded in a penny-shaped crack is reduced to the solution of the single integral equation (63). This integral equation is not amenable to solution in an exact closed form. Consequently, numerical techniques will be utilized to generate results of engineering interest.

LOAD–DISPLACEMENT RELATIONSHIP FOR THE ANCHOR

A result of particular interest to engineering applications concerns the load (P) vs displacement (Δ) relationship for the smoothly embedded anchor. Considering the integral expression for the contact stress between the anchor and the elastic medium we have

$$\sigma_{zz}^{(1)}(r,0) = \frac{1}{r} \frac{\mathrm{d}}{\mathrm{d}r} r \int_0^\infty N(\zeta) J_1(\zeta r)\,\mathrm{d}\zeta, \quad 0 < r < a. \tag{65}$$

Using the expression (38) for $N(\zeta)$ in the above equation we have

$$\sigma_{zz}^{(1)}(r,0) = \frac{2}{\pi r} F_1(r), \quad 0 < r < a. \tag{66}$$

The load–displacement relationship for the anchor plate can be evaluated by considering the equilibrium equation for the indenting plate. Assuming that the anchor displacement occurs in the direction of the applied force we have

$$P = 2\pi \int_0^a r\sigma_{zz}^{(1)}(r, 0)\,\mathrm{d}r \tag{67}$$

or

$$\frac{P}{E\Delta} = 4 \int_0^a T_1(r)\,\mathrm{d}r. \tag{68}$$

STRESS INTENSITY FACTORS AT THE BOUNDARY OF THE CRACK

The state of stress in the intact region beyond the penny-shaped crack is such that both $\sigma_{zz}^{(1)}$ $(=\sigma_{zz}^{(2)})$ and $\sigma_{rz}^{(1)}$ $(=\sigma_{rz}^{(2)})$ are nonzero for $z = 0$; $r > b$. Consequently both crack opening mode and crack shearing mode stress intensity factors are present at the crack tip. The evaluation of these stress intensity factors is important to the assessment of loads that can initiate extension of the crack tip at the attainment of some mixed mode fracture criterion.

The integral expressions for $\sigma_{zz}(r, 0)$ and $\sigma_{rz}(r, 0)$ in the region $b < r < \infty$ are given respectively by

$$\sigma_{zz}(r, 0) = \frac{2}{\pi}\left[\frac{F_2(b)}{(r^2-b^2)^{1/2}} + \int_b^r \frac{F_2'(s)\,\mathrm{d}s}{(r^2-s^2)^{1/2}}\right] \tag{69}$$

and

$$\sigma_{rz}(r, 0) = \frac{2}{\pi r^2}\frac{\mathrm{d}}{\mathrm{d}r}\int_b^r \frac{\omega S(\omega)\,\mathrm{d}\omega}{(r^2-\omega^2)^{1/2}}. \tag{70}$$

The stress intensity factors K_{I}^b and K_{II}^b at the tip of the crack are defined by

$$K_{\mathrm{I}}^b = \lim_{r\to b^+} [2(r-b)]^{1/2}\sigma_{zz}(r, 0) \tag{71}$$

and

$$K_{\mathrm{II}}^b = \lim_{r\to b^+} [2(r-b)]^{1/2}\sigma_{rz}(r, 0). \tag{72}$$

By making use of the results (69)–(72) it can be shown that

$$K_{\mathrm{I}}^b = \frac{2}{\pi}\frac{F_2(b)}{\sqrt{b}} \tag{73}$$

$$K_{\mathrm{II}}^b = \frac{2}{\pi}\frac{S(b)}{b^{3/2}}. \tag{74}$$

Alternatively, the stress intensity factors can be expressed in the integral forms in terms of $T_1(s)$ as follows:

$$\frac{K_{\mathrm{I}}^b}{E\Delta} = -\frac{2}{\pi^2}\sqrt{b}\int_0^a \frac{T_1(s)\,\mathrm{d}s}{(b^2-s^2)} \tag{75}$$

and

$$\frac{K_{\text{II}}^{b}}{E\Delta} = \frac{(1-2\nu)}{2\pi(1-\nu)b^{3/2}} \int_0^a T_1(s)\, ds. \tag{76}$$

NUMERICAL RESULTS

In order to derive results for the load–displacement behaviour of the rigid anchor plate and for the stress intensity factors at the crack tip it is necessary to obtain a solution to the governing Fredholm integral equation defined by (63). To develop a numerical solution for the integral equation we adopt the general procedures outlined by Baker (1977), Delves and Mohamed (1985) and Selvadurai *et al.* (1990, 1991). The Fredholm integral equation, in the interval $0 < r < a$ is divided into N segments with r_i ($i = 1$ to $N+1$) such that $r_i = (i-1)h$ and $h = a/N$. The equivalent matrix representation of (63) can be written as

$$[A_{ij}]\{T_1(r_j)\} = \{B_i\} \tag{77}$$

with $i, j = 1$ to N; $B_i = -1/2(1-\nu^2)$ and the coefficients A_{ij} are given by

$$A_{ij} = \begin{cases} \left\{ \dfrac{h}{\pi^2} \dfrac{K_1(r_i, r_j)}{(r_i^2 - r_j^2)} - \dfrac{(1-2\nu)^2}{8(1-\nu)^2} \dfrac{h}{b} \right\}, & \text{if } i \neq j \\[2ex] \left\{ \dfrac{1}{\pi^2} \left[\dfrac{h}{2r_i} \ln \left| \dfrac{b-r_i}{b+r_i} \right| - \dfrac{r_i h}{(b^2 - r_i^2)} \right] - \dfrac{(1-2\nu)^2}{8(1-\nu)^2} \dfrac{h}{b} \right\}, & \text{if } i = j. \end{cases} \tag{78}$$

Upon solution of the matrix equation (77), the required results for the load–displacement response (68), the stress intensity factors (75) and (76) can be obtained by using the

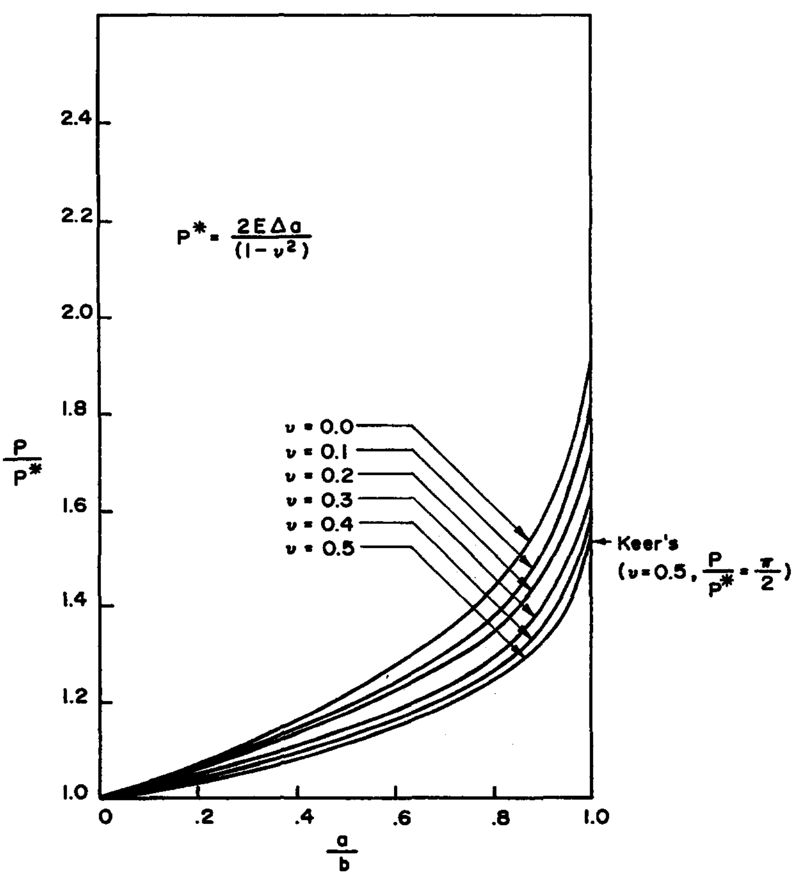

Fig. 3. Variation of the axial stiffness of the anchor plate with the extent of cracking.

discretized solution for $T_1(r)$. The solution converges very quickly and a discretization of $N = 10$ is sufficient to obtain results which compare favourably (to within an error of 1%) with certain known exact solutions for limiting cases.

It is also of interest to assess the relevance and accuracy of the numerical results by examining the results for certain limiting solutions for the problem posed in the paper.

1. In the limiting case when $(b/a) \to \infty$, the continuity constraints imposed by the uncracked region between the two halfspace regions will have no influence on the load–displacement response of the anchor plate. In this case, the load–displacement relationship for the anchor plate is given by Boussinesq's result [see, for example, Gladwell (1980)] for the smooth indentation of a halfspace region by a rigid circular indentor, i.e.

$$\frac{P}{E\Delta a} = \frac{2}{(1-\nu^2)}. \tag{79}$$

2. In the limiting case when $(b/a) \to 1$, the problem reduces to that of the smooth indentation of a penny-shaped crack of radius a by a rigid plate of equal radius. It is possible to examine the limiting case in the light of the result given by Keer (1975) and Selvadurai (1994) to the problem of a rigid disc inclusion which is embedded in bonded contact with a penny-shaped inclusion of equal radius. Keer's result (1975) for the load–displacement relationship for this problem is given by the exact closed form solution

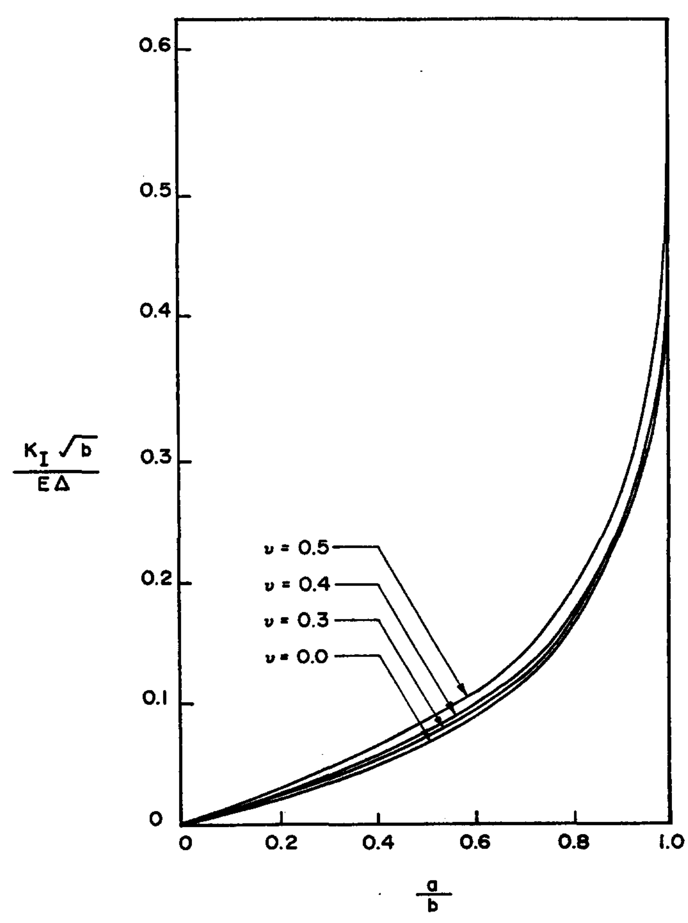

Fig. 4. Variation of the crack opening mode stress intensity factor at the boundary of the cracked region.

$$\frac{P}{E\Delta a} = \frac{2\pi}{(1+\nu)(3-4\nu)}\left[1+\frac{\{\ln(3-4\nu)\}^2}{\pi^2}\right]. \tag{80}$$

In the particular case when $\nu = 1/2$, the solution to the case of the fully bonded rigid plate coincides with the result for the case when the interface is smooth.

Figure 3 illustrates the results for the normalized value of the axial stiffness of the partially indenting anchor plate P/P^*, where $P^* = 2E\Delta a/(1-\nu^2)$. In the special case when $\nu = 1/2$, the result for P/P^* derived from the solution of the integral equation (63) agrees with the exact closed-form solution (80) given by Keer (1975). Also as $(a/b) \to 0$, the result derived from the solution of the integral equation agrees with Boussinesq's result. These numerical results also indicate that both Poisson's ratio and the anchor plate–crack aspect ratio has a significant influence on the axial stiffness of the anchor plate. Figure 4 illustrates the influence of Poisson's ratio and a/b on the flaw opening mode stress intensity factor at the crack tip. As is evident the stress intensity factor reduces to zero when the crack tip is remote from the anchor plate. The maximum value of K_I occurs when $a/b \to 1$. Analogous results for the crack shearing mode stress intensity factor are shown in Fig. 5. These results indicate that, in general, $K_{II}/K_I \ll 1$ and that when $a/b \to 1$, K_{II}/K_I has a maximum value of approximately 0.3, for $\nu = 0$. When $\nu = 1/2$. the crack shearing mode stress intensity factor is identically equal to zero. The major mode of the extension of the crack is expected to be self similar with extension taking place at the attainment of a critical value of the crack opening mode stress intensity factor.

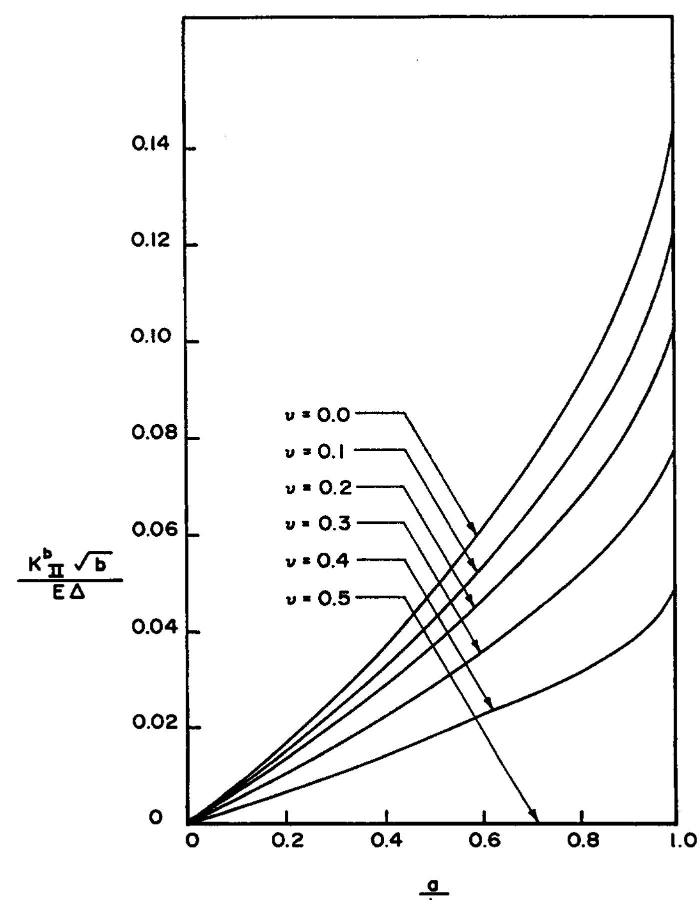

Fig. 5. Variation of the crack shearing mode stress intensity factor at the boundary of the cracked region.

CONCLUSIONS

The elastostatic problem related to the smooth indentation of the single surface of a penny-shaped crack by an embedded rigid circular anchor plate is examined. The analysis of the indentation problem can be reduced to the solution of a single Fredholm integral equation of the second kind. This equation can be solved via a numerical technique to develop results of engineering interest. The accuracy of the numerical procedure is verified by appealing to exact solutions available in the literature. Numerical results presented in the paper illustrates the manner in which the axial stiffness of the anchor plate and the stress intensity factors at the crack tip are influenced by Poisson's ratio of the elastic medium and the crack–anchor plate aspect ratio. The effect of debonding at one surface of the plate anchor has a considerable influence on the elastic compliance of the plate anchor. A comparison with results given in Selvadurai (1989) indicates that $[P/16G\Delta a]^{\text{complete bonding}}/[P/16G\Delta a]^{\text{partial bonding}}$ can vary for example, from 2 ($a/b = 0$; $\nu = 0.5$) to 1.39 ($a/b = 1$; $\nu = 0$). It is likely that even for deeply embedded anchor plates the local compliance can induce detachment of the anchor plate which can result in the attainment of a higher compliance. This aspect of deeply embedded anchor plates merits further study. Also, it is observed that the crack opening mode stress intensity factor is considerably larger than the crack shearing mode stress intensity factor for all choices of $\nu \in (0, 0.5)$ and $a/b \in (0, 1)$. Consequently, the extension of the crack due to anchor plate loading is likely to be dominated by the crack opening in the plane of the disc anchor.

REFERENCES

Baker, C. T. H. (1977). *The Numerical Treatment of Integral Equations*. Clarendon Press, Oxford.

Delves, L. M. and Mohamed, J. L. (1985). *Computational Methods for Integral Equations*. Cambridge University Press, Cambridge.

Gladwell, G. M. L. (1980). *Contact Problems in the Classical Theory of Elasticity*. Sijthoff & Noordhoff, Leyden.

Hunter, S. C. and Gamblen, D. (1974). The theory of a disc ground anchor buried in an elastic soil either with or without adhesion. *J. Mech. Phys. Solids* **22**, 371–399.

Keer, L. M. (1975). Mixed boundary value problems for a penny-shaped cut. *J. Elasticity* **5**, 89–98.

Love, A. E. H. (1927). *A Treatise on the Mathematical Theory of Elasticity*. Cambridge University Press, London.

Rowe, R. K. and Booker, J. R. (1979). A method of analysis of horizontally embedded anchors in an elastic soil. *Int. J. Numer. Anal. Meth. Geomech.* **3**, 187–203.

Rowe, R. K. and Davis, E. H. (1982). The behaviour of anchor plates in clay. *Geotechnique* **32**, 9–23.

Selvadurai, A. P. S. (1976). The load–deflexion characteristics of a deep rigid anchor in an elastic medium. *Geotechnique* **26**, 603–612.

Selvadurai, A. P. S. (1979). An energy estimate of the flexural behaviour of a circular foundation embedded in an isotropic elastic medium. *Int. J. Numer. Anal. Meth. Geomech.* **3**, 285–292.

Selvadurai, A. P. S. (1980). The eccentric loading of a rigid circular foundation embedded in an isotropic elastic medium. *Int. J. Numer. Anal. Meth. Geomech.* **4**, 121–129.

Selvadurai, A. P. S. (1984). Elastostatic bounds for the stiffness of an elliptical disc inclusion embedded at a transversely isotropic bi-material interface. *J. Appl. Math. Phys.* **35**, 13–23.

Selvadurai, A. P. S. (1989). The influence of boundary fracture on the elastic stiffness of a deeply embedded anchor plate. *Int. J. Numer. Anal. Meth. Geomech.* **13**, 159–170.

Selvadurai, A. P. S. (1993). The axial loading of a rigid circular anchor plate embedded in an elastic halfspace. *Int. J. Numer. Anal. Meth. Geomech.* **17**, 343–353.

Selvadurai, A. P. S. (1994). A contact problem for a smooth rigid disc inclusion in a penny-shaped crack. *J. Appl. Math. Phys.* **45**, 166–173.

Selvadurai, A. P. S. and Au, M. C. (1986). Generalized displacements of a rigid elliptical anchor embedded at a bi-material geological interface. *Int. J. Numer. Anal. Meth. Geomech.* **10**, 633–652.

Selvadurai, A. P. S., Au, M. C. and Singh, B. M. (1990). Asymmetric loading of an externally cracked elastic solid by an in-plane penny-shaped inclusion. *Theoret. Appl. Fracture Mech.* **14**, 253–266.

Selvadurai, A. P. S. and Nicholas, T. J. (1979). A theoretical assessment of the screw plate test. *Proc. 3rd Int. Conf. on Num. Methods in Geomech.*, Vol. 3, pp. 1245–1252. Aachen.

Selvadurai, A. P. S. and Singh, B. M. (1985). The annular crack problem for an isotropic elastic solid. *Quart. J. Mech. Appl. Math.* **38**, 233–243.

Selvadurai, A. P. S., Singh, B. M. and Au, M. C. (1991). The in-plane loading of a rigid disc inclusion embedded in an elastic halfspace. *J. appl. Mech., Trans. ASME* **58**, 362–369.

Sneddon, I. N. (1977). *Application of Integral Transforms in the Theory of Elasticity*, CISM Courses and Lectures, No. 220. Springer, Vienna.